Supplementary Materials

Cyanogel-Based Preparation of Amorphous NiFe Nanoaggregates with Enhanced Activity and Stability for OER

Shun Li[†,1], Jinxin Wan[†,1], Zhenyuan Liu[1,*], Mengdie Zhuang[1], Pengyuan Ren[2,*], Weilong Shi[1], Xiaojun Zeng[3], Jun Yang[1,*]

[1] School of Materials Science and Engineering, Jiangsu University of Science and Technology, Zhenjiang 212100, China

[2] School of Civil Engineering and Architecture, Jiangsu University of Science and Technology, Zhenjiang 212100, China

[3] School of Materials Science and Engineering, Jingdezhen Ceramic University, Jingdezhen 333403, China

* Corresponding author: zhenyuanliu@just.edu.cn (Z.L.); renpengyuan@just.edu.cn (P.R.); iamjyang@just.edu.cn (J.Y.)

[†] These authors contributed equally to this paper.

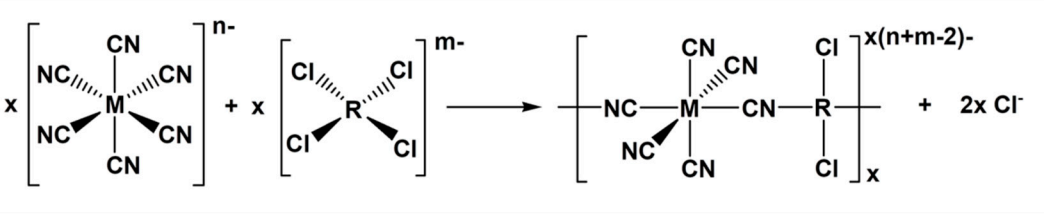

Equation S1. Formation equation of cyanogel from transition metal cyanometalates and tetrachlorometalates in aqueous solution.

$$2Ni^{2+} + Fe^{2+} + 6BH_4^- + 18H_2O \rightarrow Ni_2Fe + 6B(OH)_3 + 21H_2$$

Equation S2. Equation of chemical reaction between cyanogel and $NaBH_4$.

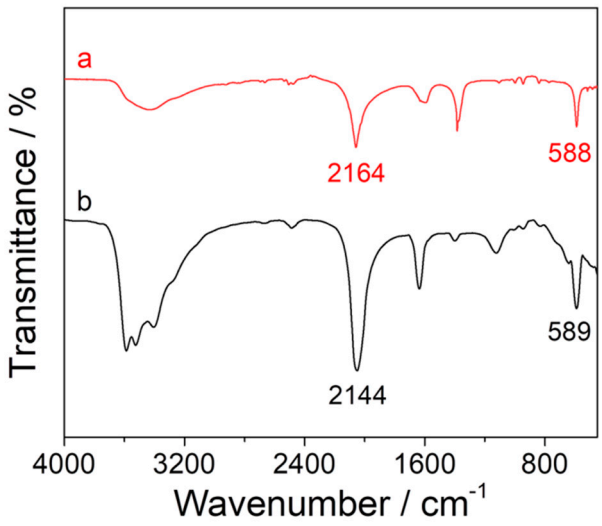

Figure S1. FT-IR spectra of (a) the $NiCl_2/Na_4Fe(CN)_6$ cyanogel and (b) pure $Na_4Fe(CN)_6$.

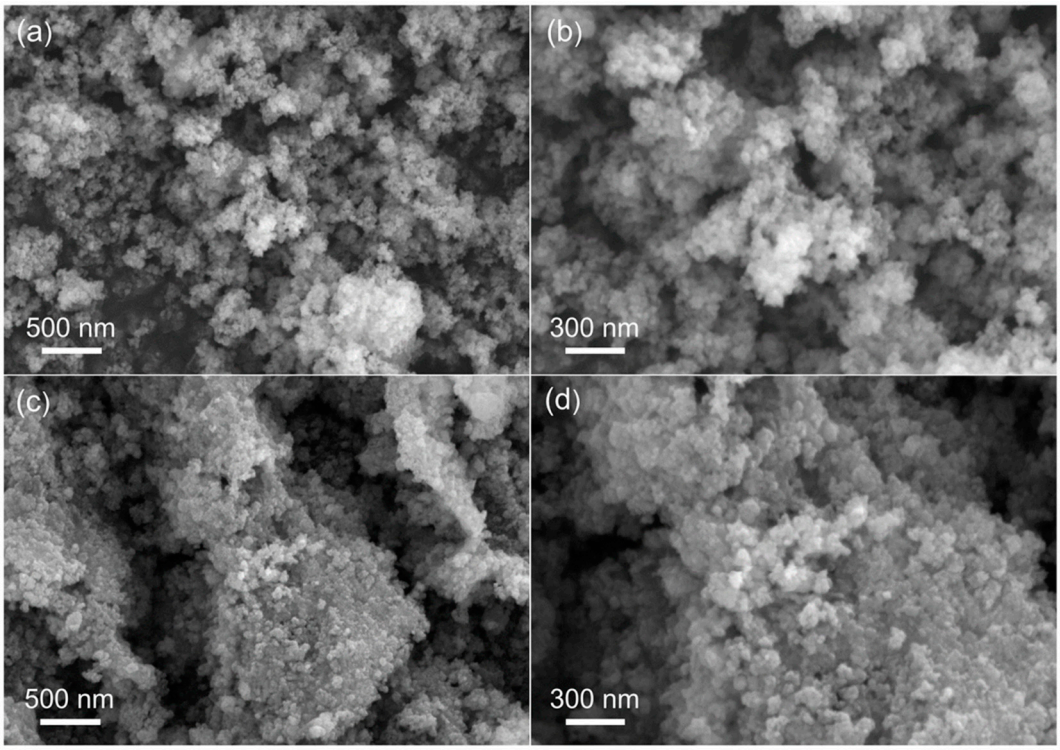

Figure S2. SEM images of (a-b) the NiFe-11 catalysts and (c-d) the NiFe-31 catalysts.

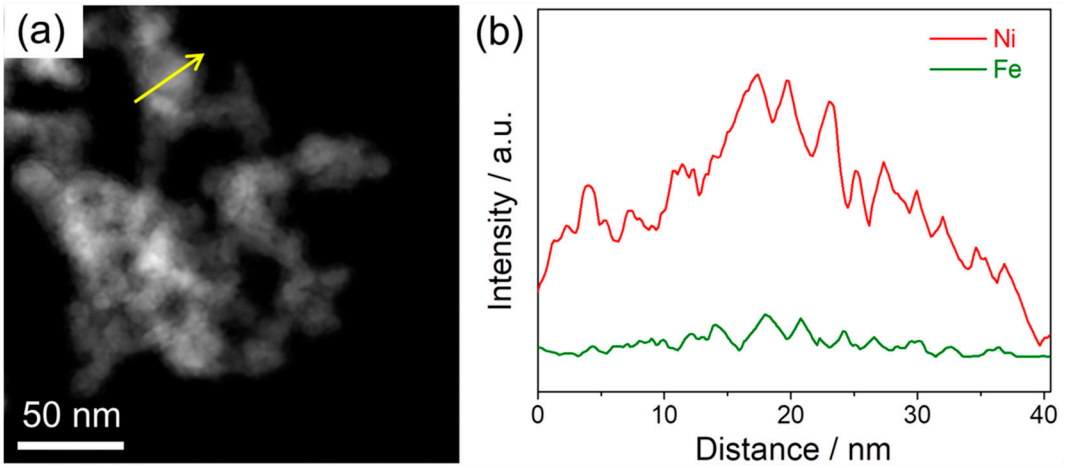

Figure S3. (a) STEM image and (b) EDX line scanning profile of the NiFe nanoaggregates.

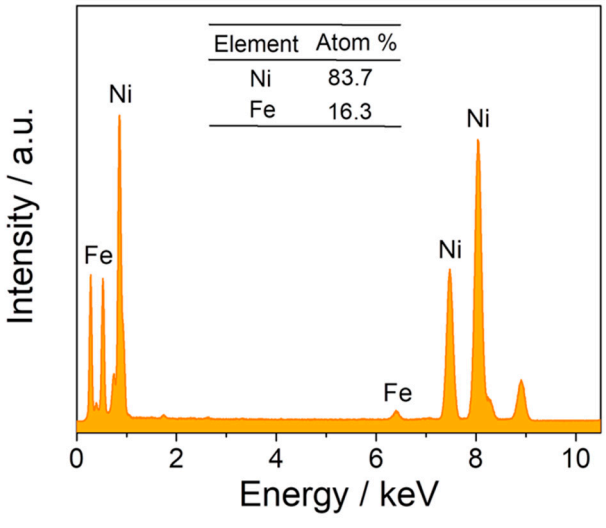

Figure S4. EDX spectrum of the NiFe-21 nanoaggregates.

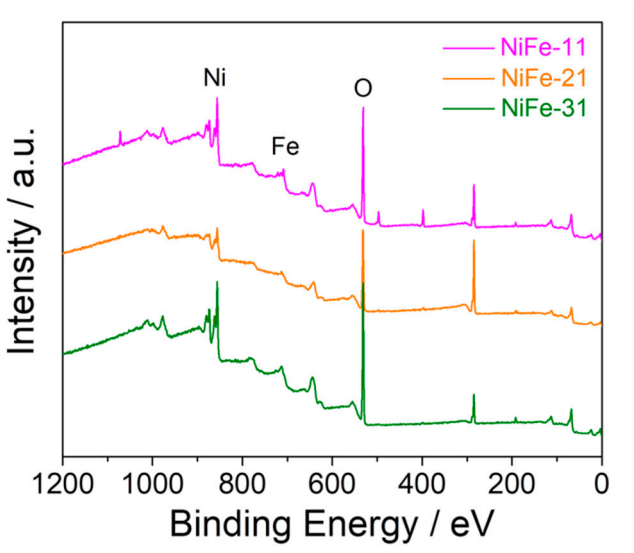

Figure S5. XPS survey scan spectra of the NiFe catalysts with different Ni/Fe molar ratio.

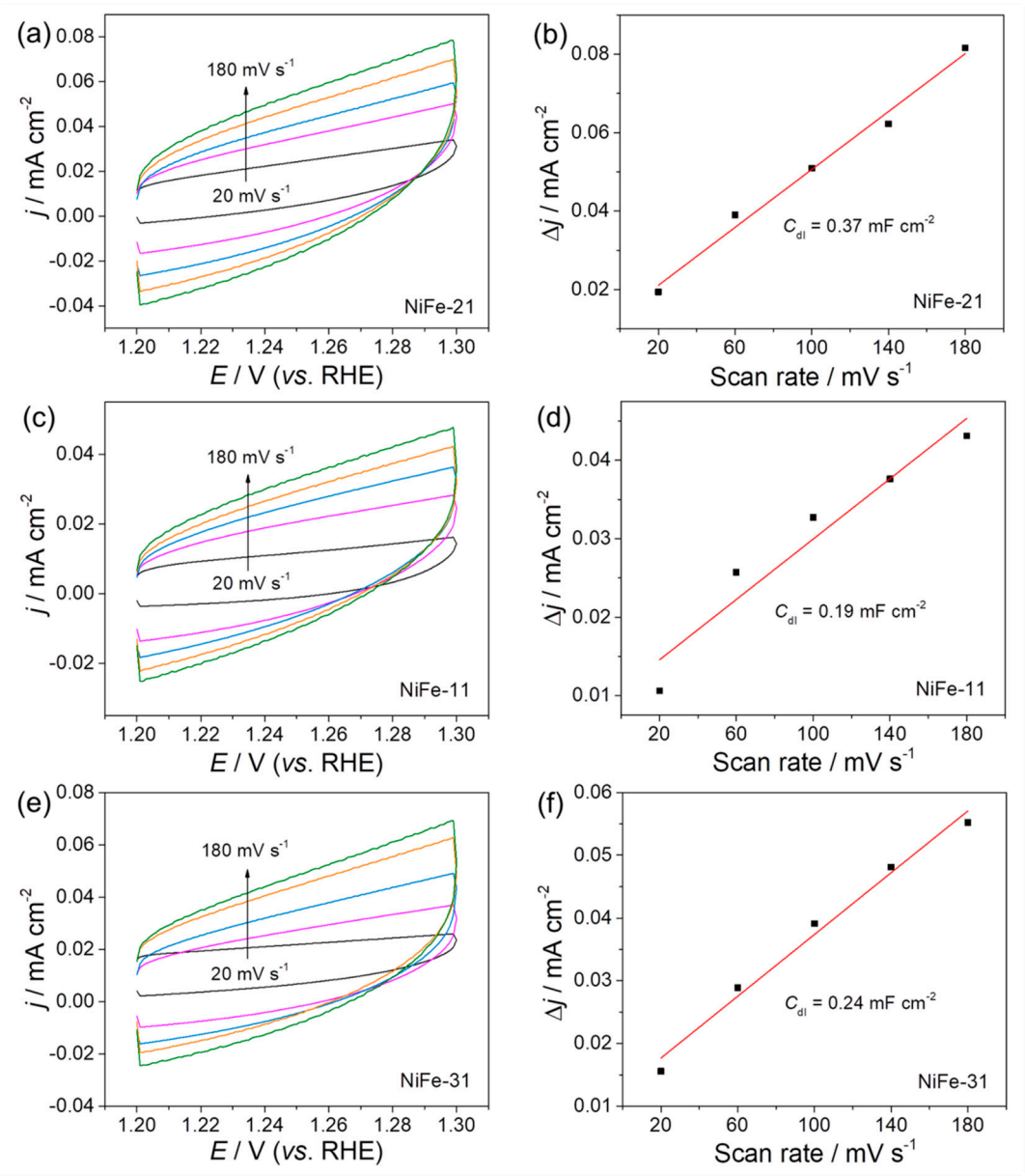

Figure S6. (a), (c) and (e) CV curves of NiFe-21, NiFe-11, NiFe-31 at different scan rates in 1 M KOH. (b), (d) and (f) Plots of the capacitive current density at 1.23 V against the scan rate of the NiFe-21, NiFe-11, NiFe-31.

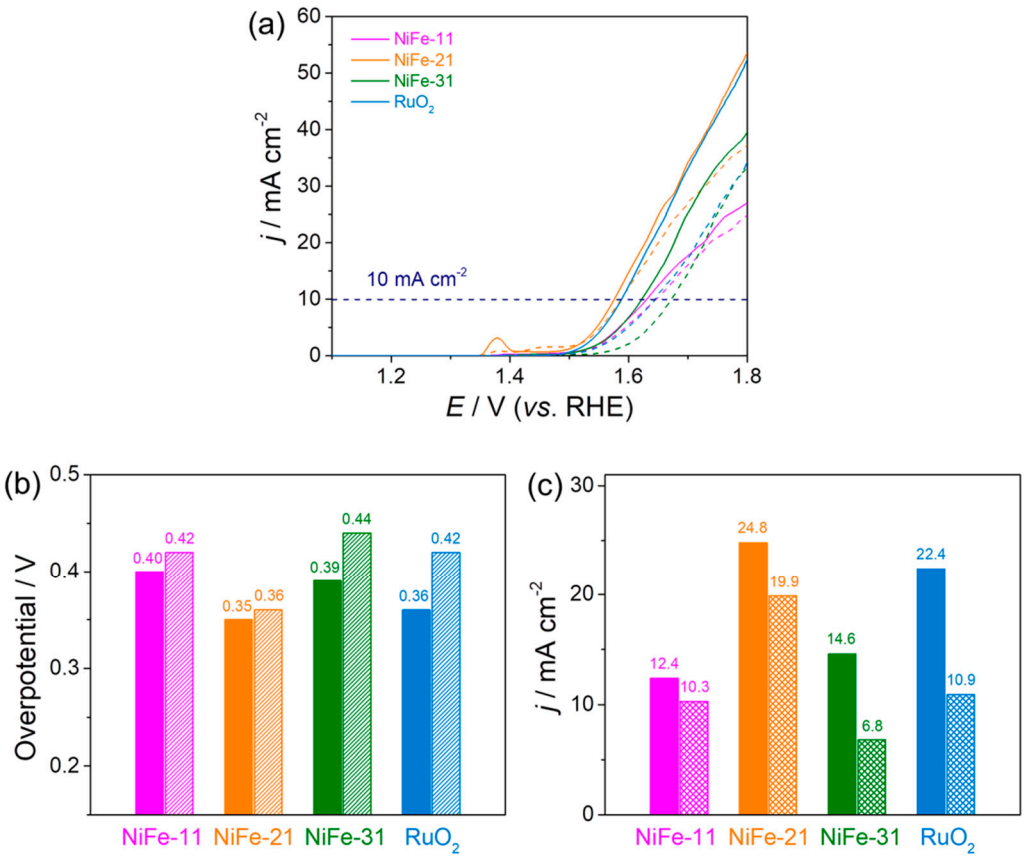

Figure S7. (a) OER polarization curves before and after 5000 cycles of the NiFe-21, NiFe-11, NiFe-31 and commercial RuO_2 catalysts. (b) Comparison of the overpotentials at the current density of 10 mA cm^{-2} before and after 5000 cycles. (c) Comparison of the current density at the potential of 1.65 V before and after 5000 cycles.

Table S1. The atomic contents of Ni and Fe in the NiFe-11, NiFe-21 and NiFe-31 nanocatalysts obtained from the full XPS results.

Catalyst	Ni / %	Fe / %
NiFe-11	12.98	7.32
NiFe-21	15.81	5.46
NiFe-31	18.83	4.05

Table S2. Comparison of the OER activity of the amorphous NiFe-21 nanoaggregates in 1 M KOH electrolyte with other electrocatalysts previously reported.

Catalyst	Overpotential / V ($10\ mA\ cm^{-2}$)	Ref.
NiFe-21	0.35	this work
NiFe-11	0.40	this work
NiFe-31	0.39	this work
NiCo-LDH	0.37	[42]
β-$Ni(OH)_2$ plates	0.44	[43]
$NiCo_2S_4$/RGO	0.36	[44]
CoNi-LDH	0.37	[45]
$NiCo_2O_4$/CNT	0.39	[46]
Ni_xCo_3-xO_4	0.42	[47]
FeNC/Ni	0.39	[48]
Co_3O_4@NiFe-LDH	0.35	[49]
NiFeC LDH	0.36	[50]
RuO_2	0.36	this work